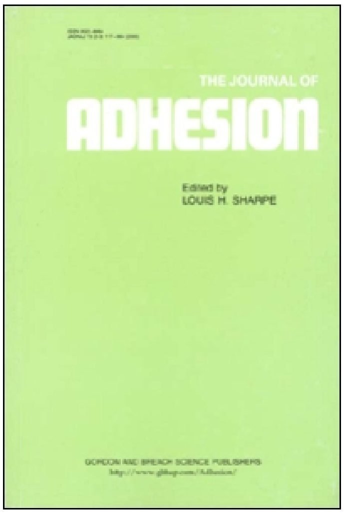

The Journal of Adhesion
Publication details, including instructions for authors and subscription information:
http://www.informaworld.com/smpp/title~content=t713453635

Particle Adhesion in Model Systems: 16. Barium Sulfate Particles on Glass and Protein Surfaces

Gary Pozarnsky[a]; Egon Matijević[a]
[a] Center for Advanced Materials Processing, Clarkson University, Potsdam, NY, USA

To cite this Article Pozarnsky, Gary and Matijević, Egon(1997) 'Particle Adhesion in Model Systems: 16. Barium Sulfate Particles on Glass and Protein Surfaces', The Journal of Adhesion, 63: 1, 53 — 69

To link to this Article: DOI: 10.1080/00218469708015213

URL: http://dx.doi.org/10.1080/00218469708015213

J. Adhesion, 1997, Vol. 63, pp. 53–69
Reprints available directly from the publisher
Photocopying permitted by license only

Particle Adhesion in Model Systems: 16. Barium Sulfate Particles on Glass and Protein Surfaces*

GARY POZARNSKY and EGON MATIJEVIĆ**

Center for Advanced Materials Processing,
Clarkson University, Potsdam, NY 13699-5814, USA

(Received 30 November 1995; In final form 15 February 1996)

The adhesion phenomena of monodispersed barium sulfate ($BaSO_4$) particles on gelatin-coated glass beads were evaluated using the packed column technique and compared with the same system in the absence of the protein.

Multilayer deposition was observed with the uncoated glass beads at pH 4, 5 and 6, while at pH 9, which is above the isoelectric point (pH $\sim$ 6) of $BaSO_4$ particles, monolayer deposition took place, even though the $BaSO_4$ particles and glass beads bore the same sign of charge. At pH = 10, no uptake was observed on the glass beads, but the addition of 10^{-4} mol dm^{-3} $BaCl_2$ induced multilayer deposition due to the adsorption of the Ba^{2+} cation on $BaSO_4$ particles, which causes a reversal of their charge to positive.

The formation of multilayers was found to occur over a much wider pH range on the gelatin coated glass beads.

$BaSO_4$ particles deposited in multilayers could not be removed from either glass beads or gelatin-coated glass beads by rinsing the loaded column with solutions of pH 11.5, but could be detached from monolayers on glass beads only.

Keywords: Adhesion of particles; detachment of particles; $BaSO_4$ particles; adhesion on gelatin; multilayer formation; packed column

1. INTRODUCTION

The kinetics of fine particle deposition from dispersions in liquids onto solid substrates, and of their detachment processes from these

---

*One of a Collection of papers honoring Robert J. Good, the recipient in February 1996 of *The Adhesion Society Award for Excellence in Adhesion Science, sponsored by 3M.*

**Corresponding author.

surfaces, are strongly influenced by forces acting in colloid systems [1–5]. The theoretical analysis of the results is facilitated by the use of monodispersed particles, which allows for the quantification of the experimentally observed attachment-detachment phenomena. The packed column technique employed in such studies is especially convenient, as it makes it possible to investigate ionic strength effects, which may lead to multi-layer deposition of adhered particles [6–19]. The latter behavior can be accounted for by considering forces that act between the adhered particles and the substrate (heterosystems) and those between already deposited particles with additional ones arriving at the surface (homosystems) [17–20].

The objective of this work was to investigate the deposition and removal characteristics of monodispersed $BaSO_4$ particles on clean and gelatin-coated glass beads using the packed column technique. The described model system is chosen to elucidate the adhesion phenomena of particles in contact with living tissues or biocompatible surfaces, which is of interest in medical diagnostics and drug delivery processes, as well as in other applications involving fine particle interactions with biological materials.

2. EXPERIMENTAL

2.1. Materials

The suspensions containing uniform ellipsoidal $BaSO_4$ particles (length ~ 200 nm, width ~ 160 nm, Fig. 1) were obtained by aging for one day at ambient temperature a 16 vol% ethanol-water solution containing 0.010 mol dm^{-3} $BaCl_2$, 0.010 mol dm^{-3} ethylenediamine tetraacetic acid (EDTA), 0.01 mol dm^{-3} Na_2SO_4, and 5 vol% of an ammonia-ammonium-chloride buffer solution ($pH = 10$) [21–23]. The solids were then filtered, washed, and evaluated by x-ray diffraction, and their particle size distribution was obtained from electron micrographs.

The number concentration was determined from the solid weight content and the density of $BaSO_4$ (4.5 gm cm^{-3}). The working dispersion had a concentration of 4.2×10^9 particles per cm^3 and its pH was adjusted with reagent grade HCl and NaOH, as needed.

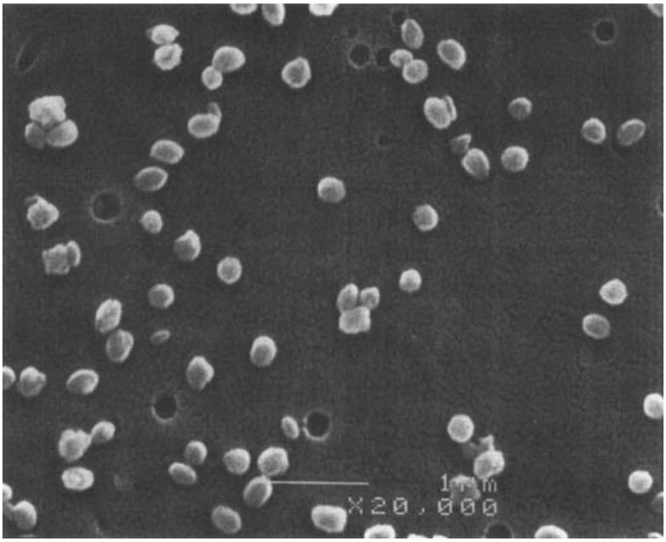

FIGURE 1 Scanning electron micrograph (SEM) of $BaSO_4$ particles prepared by aging a 16 vol% ethanol-water solution containing 0.010 mol dm^{-3} $BaCl_2$, 0.010 mol dm^{-3} EDTA, 0.010 mol dm^{-3} Na_2SO_4 and 5 vol% ammonium chloride-ammonium buffer for one day at room temperature.

An ultrapure acid-hydrolyzed pigskin gelatin (Knowledge Inc., Fort Worth, TX) was used to prepare a 0.5 wt% stock solution by gently heating the protein in water. The molecular weight and radius of gyration of this protein were experimentally determined by light scattering to be $\sim 10^6$ g/mole and 400 nm, respectively.

2.2. Packed Column

The experimental set-up was the same as used previously [19, 20]. The cylindrical column consisted of a jacketed glass cylinder having an inside diameter of 1.0 cm. The outer jacket was connected to a thermostated circulation bath to maintain the temperature at 25.0 ± 0.1°C. The column was filled with glass beads (Lapine, with a radius $r_b = 55$ μm) yielding a void volume ratio $\phi = 0.36$. The height of the packed bed was 1.5 ± 0.1 cm. The fluid flow through the bed was kept constant at 1.6 cm^3 min^{-1} by means of a peristaltic pump.

2.3. Electrokinetics

The electrokinetic mobilities of $BaSO_4$ particles were measured with DELSA 440 (Coulter Electronics) and Pen Kem 3000 instruments. Zeta potentials were calculated from these data using the MOBILITY computer program [24, 25], which includes corrections for the electrophoretic retardation and relaxation effects. The ζ-potentials of the coated and uncoated glass beads were determined previously [20]. Since the $BaSO_4$ particles are ellipsoidal, an averaged, equivalent radius of a sphere was calculated from the major and minor axes to approximate the particle flow behavior [26]. The resulting value of $r_p = 80$ nm was used in numerical calculations.

2.4. Adhesion Experiments

The packed bed was rinsed for 1 hour with an electrolyte solution of the same pH and ionic strength as that of the suspension. For experiments involving gelatin, a 0.5 wt% solution containing the protein was passed through the column for 1 hour before the bed was rinsed again with the electrolyte solution as before. Once the column was pretreated, a $BaSO_4$ dispersion of the same pH and electrolyte content was passed through the packed bed. The concentration of the particles in the effluent stream was monitored as a function of time using the intensity of scattered light at an angle of 90°. It was established experimentally that this intensity was linearly dependent on the number concentration of dispersed particles.

For removal experiments, a known amount of $BaSO_4$ particles was deposited on the glass or gelatin-coated beads in the column, which was rinsed for 20 minutes with a solution of the same pH as the initial dispersion to remove any unattached particles. A solution of pH 11.5 was then passed through the column for 2 hours. The concentration of detached particles (if any) in the effluent was assayed as before.

3. THEORETICAL

The deposition of particles is discussed in terms of a multilayer adhesion model described in detail previously [17–20], which is based on the transport of colloidal particles by convective diffusion only, assuming that the thermal energy significantly exceedes the kinetic energy ($k \gg 1/2\ mv^2$). This multilayer model has several advantages over other deposition schemes, such as those employing random sequential adsorption (RSA) mechanics [27], which only describe monolayer formation.

This multilayer model includes three parameters, two of which are mass transfer coefficients and the third relates to the area occupied per particle. The first parameter, $k_{n=1}$, describes the deposition of particles on the bare collector surface, *i.e.*, the adhesion of particles in the first layer, while $k_{n>1}$ describes the attachment of subsequent particles to the first adhered layer (multilayer formation). The third parameter $a = 1/\Gamma_{\text{max}}$, where Γ_{max} is the maximum surface concentration of particles in the first adhered layer. This parameter has the unit of area per particle, and is normalized by its own projected area, πr_p^2. The two mass transfer coefficients are normalized by the theoretically calculated mass transfer coefficient k_{th}, for the transport in a bed of packed spheres, defined by [28–33]:

$$k_{th} = 0.624 D^{2/3}\, r_p^{-2/3}\, (A_s u)^{1/3}. \tag{1}$$

where D is the diffusion coefficient of the particle of radius, r_p, u is the superficial velocity, *i.e.*, the volumetric flow rate/(column cross-sectional area times the bed porosity, ϕ), and

$$A_s = 2[1-(1-\phi)^{5/3}]/[2-3(1-\phi)^{1/3} + 3(1-\phi)^{5/3} - 2(1-\phi^2). \tag{2}$$

The three normalized parameters are then:

$$\alpha = k_{n=1}/k_{th},\ \beta = k_{n>1}/k_{th},\ \gamma = 1/\pi r_p^2\, \Gamma^{(1)}_{\text{max.}} \tag{3}$$

Ideally, the parameters α and β are independent of the fluid viscosity, particle and collector bead sizes, and bed porosity in the column. The blocking efficiency, γ, is independent of the particle size, and related to the relative surface coverage, θ, by $1/\theta_{\text{max}}$.

The particle number concentration in the effluent of the column is given by [17]:

$$\frac{C}{C_o} = \frac{(\alpha-\beta)[1-\exp(-\alpha a k_{th} C_o G)] + \alpha\beta a k_{th} C_o G}{(\alpha-\beta)[1-\exp(-\alpha a k_{th} C_o \tau)] + \alpha\beta k_{th} C_o \tau} \tag{4}$$

where C_o is the particle number concentration at the column inlet and G is a quantity that incorporates the mass balance between the suspended and adhered particles in the column. G can be obtained numerically from:

$$\frac{\partial G}{\partial x} = -\beta f k_{th} G - \frac{(\beta-\alpha)}{\alpha a C_o}[\exp(-\alpha a k_{th} C_o G) - 1] \tag{5}$$

using a fourth-order Runge-Kutta method as described previously [17–20, 34]. The column breakthrough variables, x and τ, used in expressions (4) and (5) are defined as:

$$x = z/u \quad \text{and} \quad \tau = t - (z/u) \tag{6}$$

where z is the coordinate along the cylinder axis, with $z = 0$ at the inlet and $z = z_o$ at the outlet. The deposition time, t, is counted from the moment the dispersion reaches the top of the column. The parameter f characterizes the bead surface area to void volume ratio per unit column volume and is defined as:

$$f = 3(1-\phi)/\phi r_b \tag{7}$$

The initial conditions to solve the $G(x,t)$ differential equation are $G(0,\tau) = \tau$, at $x = 0$, and $x = z_o/u$ [17–20].

The parameters α, β, and γ are obtained by comparing an experimental set of data with a set of calculated data, while simultaneously varying all three parameters to yield the best fit by a Levenberg-Marquardt scheme for non-linear curve-fitting [34], the accuracy of which was described earlier [17, 34].

4. RESULTS

4.1. Particle Characterization

X-ray diffraction patterns of the prepared $BaSO_4$ powders agreed with those listed in the powder diffraction files, confirming the crystalline nature of the particles used in the study.

The zeta potentials of the suspended $BaSO_4$ particles, and of the glass beads with and without the gelatin coating, as a function of the pH are shown in Figure 2. The opposite sign of charge is noted for $BaSO_4$ particles at $pH < 6$ and for the gelatin-coated glass beads at $pH < \sim 4.5$.

Since Ba^{2+} is a potential-determining ion for $BaSO_4$ [35], zeta potentials of the particles were also determined as a function of the concentration of added $BaCl_2$ at constant $pH = 10$. Figure 3 shows that this counterion greatly affects the particle charge, which reverses to positive at $[Ba^{2+}] = 5 \times 10^{-5}$ mol dm^{-3}.

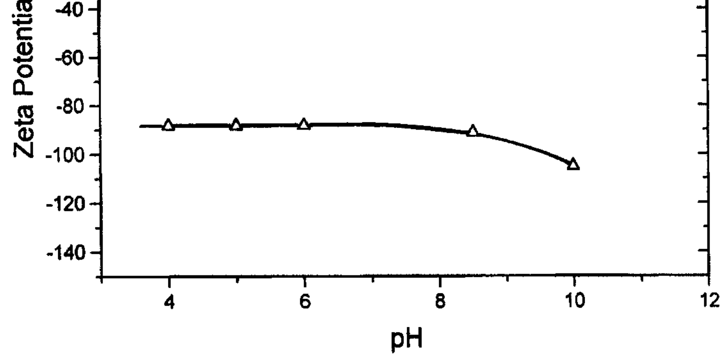

FIGURE 2 Zeta potentials of glass beads (△), of gelatin-coated beads (◇), and of $BaSO_4$ particles (○) as a function of the pH.

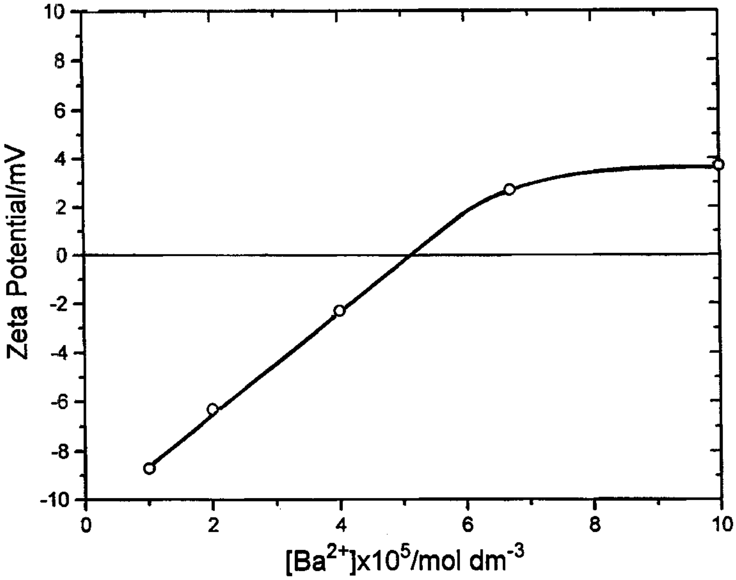

FIGURE 3 Zeta potential of $NaSO_4$ particles as a function of the molar concentration of Ba^{2+} at pH = 10.

4.2. Particle Deposition

The column breakthrough curves for the deposition of $BaSO_4$ particles on glass beads at three pH values and one Ba^{2+} cation concentration are given in Figure 4. While at pH = 10, very little attachment on the clean beads is indicated, which is confirmed by scanning electron microscopy (SEM); at pH = 9 limited uptake is observed, even though the collector and $BaSO_4$ particles bear the same sign of charge. The shape of the breakthrough curve in the latter case is characteristic of monolayer formation, which is also confirmed by the SEM (Fig. 5a).

The interaction of $BaSO_4$ particles with the oppositely-charged glass beads at pH 5 and 6 occurred too quickly to be followed by the packed column technique, but SEM examination clearly showed multilayer deposition in both cases. The deposition of $BaSO_4$ particles at pH 4 also resulted in multilayer formation, as indicated by the shape of the breakthrough curve (Fig. 4) and the corresponding electron micrograph (Fig. 5b).

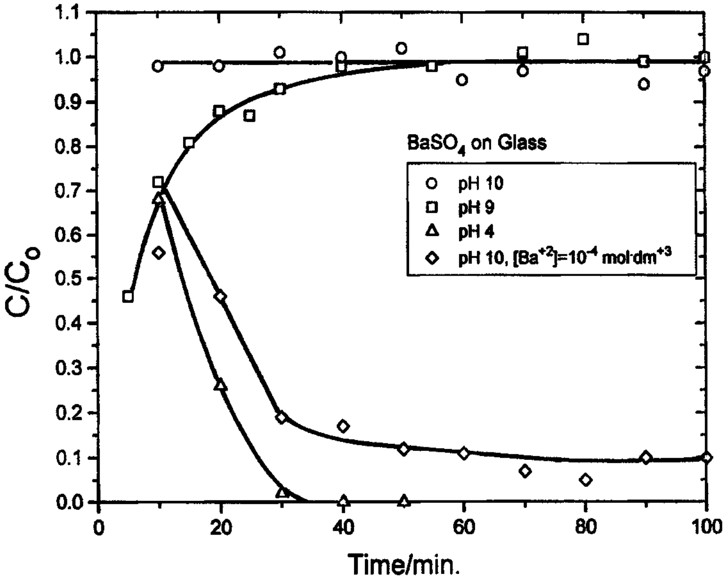

FIGURE 4 The plot of the ratios of the concentration of $BaSO_4$ particles (illustrated in Fig. 1) in the effluent (C) to the initial concentration ($C_o = 4.2 \times 10^9$ particles cm^{-3}) as a function of time for the deposition of $BaSO_4$ particles on glass beads at pH = 4(Δ), 9(□), 10(○) and pH 10 at $[Ba^{2+}] = 10^{-4}$ mol dm^{-3} (◇).

Using a $BaSO_4$ particle dispersion at pH = 10 to which 1×10^{-4} mol dm^{-3} $[Ba^{2+}]$ was added, the breakthrough curve again clearly indicates multilayer depostion (Fig. 4), as corroborated by the SEM in Figure 6a.

The uptake of $BaSO_4$ particles on the gelatin coated beads at different pH values as a function of time is shown in Figure 7, while the micrograph in Figure 6b illustrates the resulting surface after the deposition. Multilayer formation is observed over the entire pH range of 4 to 10.

4.3. Particle Detachment

Particles deposited on the glass beads in monolayers at pH 9 (Fig. 5a) could be completely removed by washing the column with aqueous solutions of pH = 11.5, which was verified by the SEM examination. In contrast, particles adhering in mutlilayers to the glass beads at pH 4

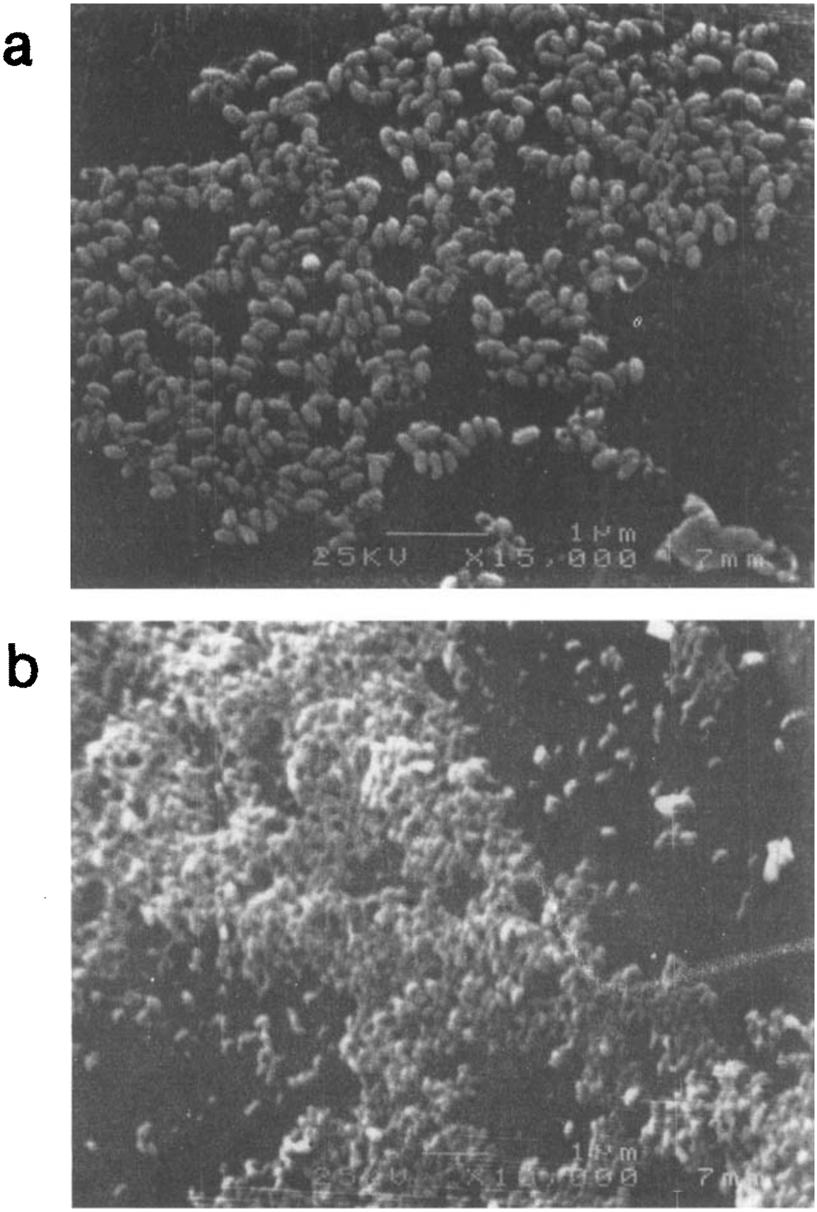

FIGURE 5 SEM of $BaSO_4$ particles on glass beads deposited at (a) pH = 9 after two hours of the dispersion flowing through the column under conditions given in Figure 4, and (b) pH = 9 on glass beads after one hour.

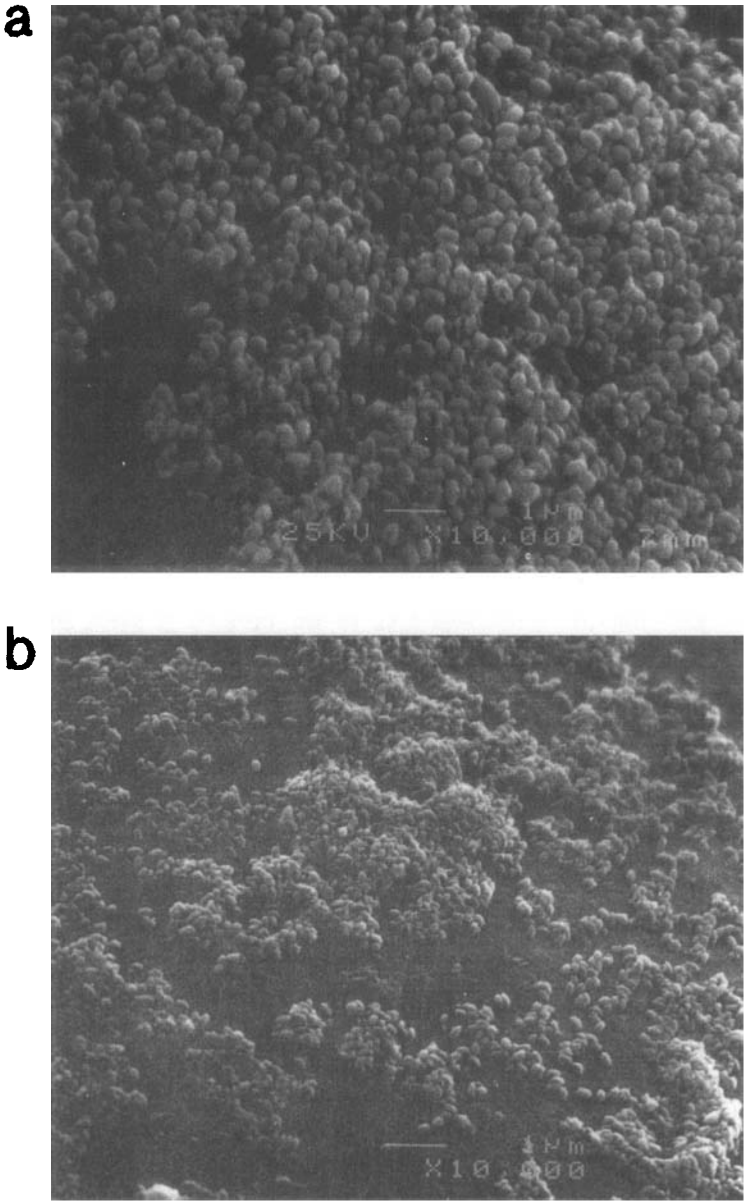

FIGURE 6 SEM of multilayers of $BaSO_4$ particles deposited on glass beads after one hour (a) under conditions given in Figure 4 at pH 10 and $[Ba^{2+}] = 10^{-4}$ mol dm^{-3}, and (b) at pH 10 with gelatin coated beads at the conditions in Figure 7.

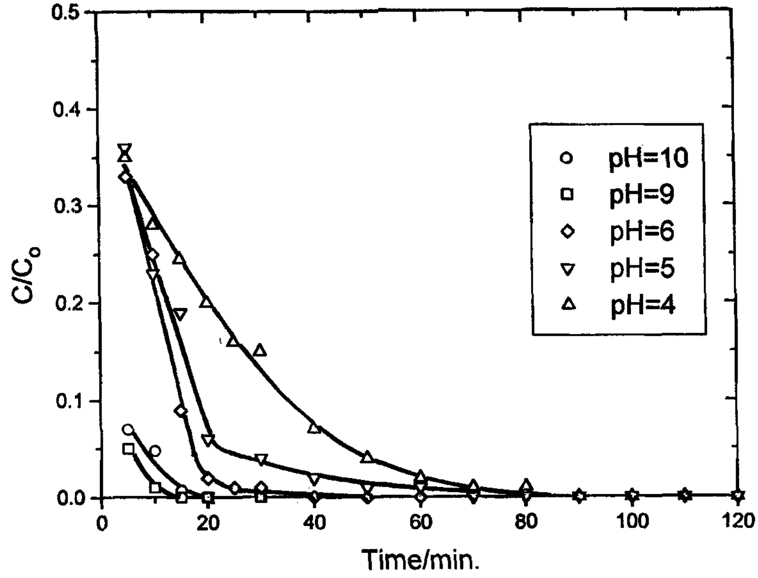

FIGURE 7 The plot of the ratio C/C_0 for the deposition of $BaSO_4$ particles ($C_o = 4.2 \times 10^9$ particles cm^{-3}) at pH = 4(△), 5(▽), 6(◇), 9(□), and 10(○) onto gelatin-coated glass beads as a function of time.

(Fig. 5b), on gelatin-coated beads at pH 10, or in the presence of $[Ba^{2+}] = 10^{-4}$ mol dm^{-3} at pH 10, could not be detached after washing with solutions of the same pH (11.5).

5. DISCUSSION

5.1. Adhesion on Glass Beads

The adhesion behavior of $BaSO_4$ particles with respect to clean glass beads can be explained by considering the charge of both interacting surfaces as a function of the pH (Fig. 2). When these charges are of the same sign and of sufficiently high magnitude, no deposition occurs (e.g., at $pH \geqslant 10$). The calculation of the total interaction energy for the $BaSO_4$/glass system, based on the Hogg, Healy, and Fuerstenau (HHF) approximation [36], at pH = 10 (ionic strength, $I = 2.0 \times 10^{-4}$ mol. dm^{-3}, Debye length, $\kappa = 5 \times 10^7 \, m^{-1}$, $r_1 = 55 \, \mu m, r_2 = 0.08 \, \mu m$,

$\psi_1 = -105\,\mathrm{mV}$, $\psi_2 = -32\,\mathrm{mV}$, Hamaker constant, $A_{132} = 1.8 \times 10^{-20}\,\mathrm{J}$) indeed shows a very high repulsion barrier, which should prevent particle deposition (Fig. 8). At pH = 9 ($I = 2.0 \times 10^{-5}$ mol.dm^{-3}, $\kappa = 1.5 \times 10^7\,\mathrm{m}^{-1}$, $\psi_1 = -92$ mV, $\psi_2 = -22$ mV), the surface potentials of the glass beads and of the $BaSO_4$ particles are lower but of the same sign, resulting in a decrease of the maximum potential energy barrier from ~150 kT to ~50 kT, and a shift of this maximum from ~20 nm to ~90 nm. The lower value of ~50 kT at pH = 9 should be sufficient to prevent adhesion, yet monolayer deposition does take place. This overestimation of the repulsion energy barrier may be due to the Derjaguin approximation of spherical geometry used in the HHF calculations [37, 38]. For values of $\kappa r_2 > \sim 5$, the spherical approximation is a good estimate of the repulsive forces between particles, while at $\kappa r_2 < 5$, the results become inaccurate. At pH ~ 10, the former condition is fulfilled, but at pH = 9, the κr_2 product is approximately unity, resulting in too high an energy barrier [39]. The calculations do not include the effects of charge segregation, which

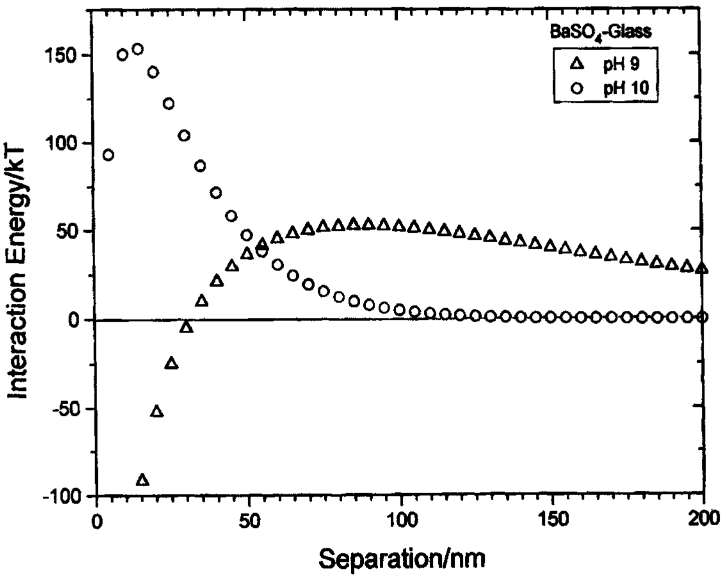

FIGURE 8 Total interaction energy as a function of the separation between $BaSO_4$ particles and glass beads at pH = 9(Δ) and 10(○) as calculated using the Hogg, Healy, Fuersteneau (HHF) approximation [36].

may also contribute to the discrepancy between the theory and experiment [40].

Close to the i.e.p. of $BaSO_4$ (at $pH = 6$), multilayer deposition is observed which is analogous to the behavior of hematite particles on glass beads at their i.e.p ($pH \sim 8.5$) [20]. At $pH = 4$ and 5 where the charges on the interacting glass beads and $BaSO_4$ particles are opposite in sign, monolayers are formed initially. Under these conditions, the $BaSO_4$ particles are still only weakly charged, leading to mutual attraction at the surface and consequent multilayer deposition (Fig. 5b).

Due to the adsorption of Ba^{2+} ions on $BaSO_4$ particles, the charge of the latter can be easily reduced or even reversed [35]. Thus, at 10^{-4} mol dm^{-3} $[Ba^{2+}]$ and $pH = 10$, the weakly charged $BaSO_4$ particles adhere to the glass in multilayers as shown in Figure 6a.

5.2. Gelatin-Coated Beads

The deposition of $BaSO_4$ particles on gelatin-coated glass beads takes place in multilayers over the entire pH range (*i.e.* 4–10) tested. This effect is most likely due to charge and chemical effects. The gelatin coating substantially lowers the potential on the glass beads. Since the $BaSO_4$ particles also show a relatively low potential, the repulsion should be rather weak. In addition, the gelatin can interact with $BaSO_4$ through bond formation either between Ba^{2+} and carboxyl groups or SO_4^{2-} and amino groups on the polymer, further enhancing the adsorbability. Similar results were obtained with the adhesion of hematite on gelatin-coated collectors [20].

A comparison of the α, β and θ_{max} parameters for the deposition of particles on the uncoated and gelatin-coated collectors is given in Table I. The corresponding values at pH 5 and 6 for the uncoated glass beads could not be calculated due to the extremely fast deposition rates at these conditions, but it can be assumed that they are much higher than those listed at pH 4, since multilayer deposition was observed over this pH range.

The values of α for the uncoated beads increase as the pH is decreased from 10 ($\alpha \sim 0$, little or no uptake of particles) to pH 4, which reflects the weaker repulsion between the $BaSO_4$ particles and glass beads as the isoelectric point (i.e.p.) of $BaSO_4$ ($pH \sim 6$) is approached.

TABLE I Values of α, β, and θ_{max} for Gelatin-Coated and Uncoated Glass Beads

	Gelatin-Coated Glass Beads			*Uncoated Glass Beads*		
pH	α	β	θ_{max}	α	β	θ_{max}
4	0.16	2.3	0.05	0.10	5.0	0.04
5	0.10	8.0	0.04	–	–	–
6	0.10	8.2	0.04	–	–	–
9	0.50	8.0	0.10	0.25	0	0.01
10	0.40	4.9	0.05	0	0	0

The value of β (multilayer deposition efficiency) also increases in the vicinity of the i.e.p. of $BaSO_4$.

For the gelatin-coated beads, the parameter β has a finite value over the entire pH range, which is consistent with the multilayer deposition confirmed by electron microscopy.

The values of θ_{max} for $BaSO_4$ deposition on glass collectors indicate that the "jamming" limit for the ellipsodial particles is lower than that for particles with spherical geometry ($\theta_{max} = 0.346$) [27], and also indicates a high amount of lateral repulsion between the $BaSO_4$ particles. Another major factor in this deposition process is the effect of "hydrodynamic scattering" [27], which causes deposition to take place mainly on the front and back of the spherical collectors, where the deposited particles experience little or no hydrodynamic shear. This is demonstrated in the various micrographs where the coverage of the $BaSO_4$ particles appears to be much greater than the corresponding θ_{max} values, which are averaged over the entire surface of the collectors.

The values of θ_{max} increase for the deposition on gelatin-coated collectors as the gelatin interacts with the $BaSO_4$ particles. This interaction neutralizes the amount of lateral repulsion between the particles and increases the value of θ_{max}.

It was demonstrated earlier that a steep increase in the values of β coincides with the critical coagulation concentration of a dispersion used in deposition experiments [19]. The values of β are also > 1, which indicates some coagulation in the particle dispersion. The electron micrographs of systems described in this work show that the "multilayers" actually consist of aggregated $BaSO_4$ particles both on glass and polymer-coated collectors. Failing to detach such particles may be due to the fact that aggregates are difficult to peptize and/or that they fill the voids between the beads, thus clogging up the column.

Acknowledgements

The authors are indebted to Nanosystems, Collegeville, PA, for supporting this work and to Dr. Niels Ryde. (Rohm & Haas, Springhouse, PA) for useful discussions.

References

[1] van de Ven, T. G. M., *Colloidal Hydrodynamics* (Academic Press, New York, 1989).
[2] Ruckenstein, E. and Prieve, D. C., *Testing and Characterization of Powders and Fine Particles* (Weydon & Sons, London, 1980).
[3] Ruckenstein, E. and Prieve, D. C., *J. Chem. Soc. Faraday Trans. 2* **69**, 1522 (1973).
[4] Spielman, L. A. and Friedlander, S. K., *J. Colloid Interface Sci.* **46**, 22 (1974).
[5] Rajagopalan, R. and Kim, J. S., *J. Colloid Inter face Sci.* **83**, 428 (1981).
[6] Adamczyk, Z., *Colloids Surf.* **39**, 1 (1989).
[7] Yao, K. M., Habibian, M. T. and O' Melia, C. R., *Environ. Sci Technol.* **5**, 1105 (1971).
[8] Fitzpatrick, J. A. and Spielman, L. A., *J. Colloid Interface Sci.* **43**, 350 (1973).
[9] Elimelech, M., *Langmuir* **6**, 1153 (1990).
[10] Elimelech, M. and O'Melia, C. R., *Environ. Sci. Technol.* **24**, 1528 (1990).
[11] Elimelech, M., *J. Colloid Interface Sci.* **146**, 337 (1991).
[12] Kolakowski, J. E. and Matijević, E., *J. Chem. Soc. Faraday Trans. 1* **75**, 65 (1979).
[13] Kuo, R. J. and Matijević, E., *J. Chem. Soc. Faraday Trans. 1* **75**, 65 (1979).
[14] Kuo, R. J. and Matijević, E., *J. Colloid. Interface. Sci.* **78**, 407 (1980).
[15] Kallay, N., Tomić, M., Biškup, B., Kunjašić I. and Matijević, E., *Colloids Surf.* **28**, 185 (1987).
[16] Matijević, E. and Kallay, N., *Croat. Chem. Acta* **56**, 649 (1983).
[17] Privman, V., Frisch, H. L., Ryde, N. and Matijević, E., *J. Chem. Soc. Faraday Trans.* **87**, 1377 (1991).
[18] Ryde, N., Kallay, N. and Matijević, E., *J. Chem. Soc. Faraday Trans.* **87**, 1377 (1991).
[19] Ryde, N., Kihira, H. and Matijević, E., *J. Colloid. Interface. Sci.* **15**, 421 (1991).
[20] Ryde, N. and Matijević, E., *J. Colloid. Interface. Sci.* **169**, 468 (1995).
[21] Takiyama, K., *Bull. Chem. Soc. Japan* **31**, 950 (1958).
[22] Petres, J., Deželić, G. and Težak, B., *Croat. Chem. Acta* **38**, 277 (1958).
[23] Suito, E. and Takiyama, K., *Bull. Chem. Soc. Japan* **28**, 305 (1995).
[24] White, L. R., Mangelsdorf, C. S. and Chan, C. Y. C., Computer program MOBILITY, Dept. of Mathematics, University of Melbourne, Parkville, Victoria 2052, Australia.
[25] O'Brien, R. W. and White, L. R., *J. Chem. Soc. Faraday Trans. 2* **74**, 1607 (1978).
[26] Perrin, F., *J. Phys. Rad.* **7**, 1 (1936).
[27] Johnson, P. R. and Elimelech, M., *Langmuir* **11**, 801 (1995).
[28] Happel, J., *AIChE J.* **4**, 197 (1958).
[29] Ruckenstein, E. and Westfried, F., *C. R. Acad. Sci. Paris* **251**, 2467 (1960).
[30] Ruckenstein, E., *Chem. Eng. Sci.* **19**, 131 (1964).
[31] Pfeffer, R. and Happel, J., *AIChE. J.* **10**, 605 (1964).
[32] Ruckenstein, E., *Ind. Eng. Chem. Fundam.* **3**, 380 (1964).

[33] Levich, V. G., *Physiochemical Hydrodynamics* (Prentice-Hall, Engelwood Cliffs, NJ, 1962).

[34] Press, W. H., Flannery, B. P., Teukolsky, S. A. and Wetterling, W. T., *Numerical Recipes* (Cambridge University Press, New York, 1986).

[35] Matijević, E. and Težak, B., *Kolloid Z.* **146**, 65 (1956).

[36] Hogg, R., Healy, T. W. and Fuerstenau, D. W., *Trans. Faraday. Soc.* **62**, 1638 (1966).

[37] Derjaguin, B., *Kolloid Z.* **69**, 155 (1934).

[38] Derjaguin, B., *Acta Physiochimica URSS* **10**, 333 (1939).

[39] Verwey, E. J. W. and Overbeek, J. Th. G., *Theory of the Stability of Lyophobic Colloids* (Elsevier, Amsterdam, 1948).

[40] Kihira, H. and Matijević, E., *Adv. Colloid Interface Sci.* **42**, 1 (1992).